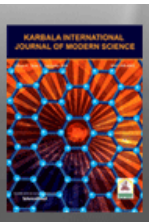

Karbala International Journal of Modern Science

Volume 11 | Issue 1 Article 2

Gauss-Lobatto Method for Nuclear Reactivity Calculation

Daniel Suescún-Díaz
Department of Natural Sciences, Avenida Pastrana, Universidad Surcolombiana, 410001, Neiva, Huila, Colombia, daniel.suescun@usco.edu.co

Luis E. Cardoso-Páez
Department of Natural Sciences, Avenida Pastrana, Universidad Surcolombiana, 410001, Neiva, Huila, Colombia

Diego Peña-Lara
Grupo de Transiciones de Fases y Materiales Funcionales, Universidad del Valle, 760032, Cali, Colombia;

Recommended Citation

Suescún-Díaz, Daniel; Cardoso-Páez, Luis E.; and Peña-Lara, Diego (2024) "Gauss-Lobatto Method for Nuclear Reactivity Calculation," *Karbala International Journal of Modern Science*: Vol. 11 : Iss. 1 , Article 2.
Available at: https://doi.org/10.33640/2405-609X.3384

Gauss-Lobatto Method for Nuclear Reactivity Calculation

Abstract

In this paper, we introduce a novel approach to numerical solving for nuclear reactivity using the inverse equation of point kinetics as a model. Our method leverages the Gauss-Lobatto quadrature, incorporating multiple time steps and nodes derived from Legendre polynomials of varying orders. To enhance the accuracy of the differential component of the inverse equation, we employed a differential scheme based on the Gauss-Lobatto quadrature nodes. To address fluctuations in neutron population density, we implemented a second-order low-pass Butterworth filter with a minimal window length of $M = 3$ samples. Through extensive numerical simulations, we assessed the precision of our proposed method and filtering process by varying time steps and standard deviations associated with noise or uncertainty. Additionally, we benchmarked our results against the Savitzky-Golay filter, which uses a significantly larger sampling window of $M = 225$. Our findings reveal that the integration of the Gauss-Lobatto quadrature method with the Butterworth filter not only significantly reduces fluctuations but also demonstrates potential for effective implementation in digital reactivity meters.

Keywords

nverse point kinetic equations; Gauss-Lobatto quadrature; nuclear reactivity; Butterworth filter; Numerical simulation

RESEARCH PAPER

Gauss-Lobatto Method for Nuclear Reactivity Calculation

Daniel Suescún-Díaz [a,*], Luis E. Cardoso-Páez [a], Diego Peña-Lara [b,c]

[a] Department of Natural Sciences, Avenida Pastrana, Universidad Surcolombiana, 410001, Neiva, Huila, Colombia
[b] Grupo de Transiciones de Fases y Materiales Funcionales, Universidad del Valle, 760032, Cali, Colombia
[c] Centro de Excelencia en Nuevos Materiales (CENM), Universidad del Valle, 760032, Cali, Colombia

Abstract

In this paper, we introduce a novel approach to numerical solving for nuclear reactivity using the inverse equation of point kinetics as a model. Our method leverages the Gauss-Lobatto quadrature, incorporating multiple time steps and nodes derived from Legendre polynomials of varying orders. To enhance the accuracy of the differential component of the inverse equation, we employed a differential scheme based on the Gauss-Lobatto quadrature nodes. To address fluctuations in neutron population density, we implemented a second-order low-pass Butterworth filter with a minimal window length of $M = 3$ samples. Through extensive numerical simulations, we assessed the precision of our proposed method and filtering process by varying time steps and standard deviations associated with noise or uncertainty. Additionally, we benchmarked our results against the Savitzky−Golay filter, which uses a significantly larger sampling window of $M = 225$. Our findings reveal that the integration of the Gauss-Lobatto quadrature method with the Butterworth filter not only significantly reduces fluctuations but also demonstrates potential for effective implementation in digital reactivity meters.

Keywords: Inverse point kinetic equations, Gauss-Lobatto quadrature, Nuclear reactivity, Butterworth filter, Numerical simulation

1. Introduction

The energy in a nuclear reactor comes from a large chain of reactions involving the fission of heavy atoms such as U-235 within the reactor core. The programmed motion of the control rods can stabilize chain reactions. Moving the control rods generates variations in the density of the neutron population, which in turn causes changes in nuclear reactivity [1]. One technique used to program the motion of the control rod banks is calculating nuclear reactivity through the inverse point kinetic equation (IPKE). This method is often the primary tool for developing nuclear reactivity meters in power reactors [2]. To solve the IPKE, the density of the neutron population inside the reactor core must be known. In practice, this can be determined with measuring devices, but due to the stochastic nature of nuclear reactions within the reactor core, the data obtained from measurements have fluctuations that make the numerical calculation of nuclear reactivity complex [3].

There are different tasks in nuclear power plants, the most important of which is the safe control of the reactor through reactivity [4]. A reactivity-initiated accident is a typical nuclear reactor accident during which the core fission rate and power increase unexpectedly [5]. Research has been carried out in a BAEC TRIGA Mark-II research reactor to study the effects of reactivity insertion and in a prototype fast breeder reactor [6]. Some authors estimate reactivity on an experimental basis [7]. Typically, the model takes the neutron density as an input function and information that can be obtained with devices such as ionization chambers [8]. An accurate reactivity value can predict changes in the

Received 14 September 2024; revised 16 November 2024; accepted 19 November 2024.
Available online 14 December 2024

* Corresponding author.
E-mail address: daniel.suescun@usco.edu.co (D. Suescún-Díaz).

https://doi.org/10.33640/2405-609X.3384

neutron population density and neutron detector location [9]. A work helps to improve safety features in a nuclear reactor through reactivity [10]. In another method, the reactivity is obtained by the first-order perturbation calculations [11].

This work proposes using a recently published second-order low-pass Butterworth filter [12] in conjunction with the numerical calculation of nuclear reactivity using Gauss-Lobatto quadrature to minimize fluctuations. One of the main characteristics of this filter is its feedback term, which necessitates fewer coefficients for filtering operations, resulting in improved computational efficiency with a smaller sampling window.

2. Theoretical considerations

In the study of a nuclear reactor's dynamic behavior, a set of $m+1$ strongly coupled differential equations arises, associated with m groups of delayed neutron precursors. These equations describe the temporal behavior of the density of the neutron population and the concentration of delayed neutron precursors inside the core of a nuclear reactor.

The formalism for the point kinetics equations is obtained after making several physical assumptions from a more general equation associated with a neutron diffusion equation that describes the spatiotemporal evolution of neutron density.

The mathematical form of the point kinetic equations for six groups of delayed neutron precursors ($m=6$) can be expressed as [13],

$$\frac{dN(t)}{dt}=\left[\frac{\rho(t)-\beta}{\Lambda}\right]N(t)+\sum_{i=1}^{6}\lambda_i C_i(t) \tag{1}$$

$$\frac{dC_i(t)}{dt}+\lambda_i C_i(t)=\frac{\beta_i}{\Lambda}N(t) \tag{2}$$

where $N(t)$ represents the neutron density (proportional to the nuclear power), $C_i(t)$ is the concentration of the i-th group of delayed neutron precursors, $\rho(t)$ the reactivity, λ_i is the decay constant of the i-th group of delayed neutron precursors, β_i the effective fraction of the i-th group of delayed neutrons, β is the total effective fraction of delayed neutrons, and Λ is the neutron generation time. Equations (1) and (2) with the initial conditions $N(t=0)=N_0$ and $C_i(t=0)=\beta_i N_0/(\lambda_i\Lambda)$ allow us to find the population density and the neutron concentration at each time step.

This work will consider its inverse process when calculating nuclear reactivity. One can invert equations (1) and (2) to derive an expression for nuclear reactivity, assuming the neutron density is known. This results in an integral-differential equation [14],

$$\rho(t)=\beta+\frac{\Lambda}{N(t)}\frac{dN(t)}{dt}-\frac{\langle N_0\rangle}{N(t)}\sum_{i=1}^{6}\beta_i e^{-\lambda_i t}-\frac{1}{N(t)}\sum_{i=1}^{6}\int_0^t\lambda_i\beta_i e^{-\lambda_i(t-t')}N(t')dt' \tag{3}$$

where $\langle N_0\rangle$ is the average initial value of all fluctuating measurements before time $t_0=0$.

Equation (3) is known as the inverse equation of point kinetics, and it is a model that allows the development of digital meters of nuclear reactivity [2]. The differential part of this equation is associated with the reactor's period, and the integral part is related to the reactor's power history.

Due to the integral-differential nature of this expression, a method must be capable of solving the integral and differential parts jointly and accurately. For this reason, the construction of a numerical scheme that uses the Gauss-Lobatto quadrature is proposed.

3. Proposed method

In this section, the Gauss-Lobatto numerical integration method is presented. This method is based on interpolating polynomials with preassigned abscissas at the ends and internal points of the integration interval. It can be expressed as shown in equation (4) [15]:

$$\int_{-1}^{1}f(t)dt=\frac{2}{n(n-1)}\left[f(-1)+f(1)\right]+\sum_{j=2}^{n-1}w_j f(x_j)+E(f) \tag{4}$$

where n is the number of points that the quadrature takes to approximate the polynomial of degree $n-1$, x_i the internal evaluation points or quadrature nodes; w_j are the weight coefficients, and $E(f)$ is the term associated with the error.

The nodes x_i are given by the zeros of the polynomial resulting from the derivative of the interpolating Legendre polynomial $P_n(x)$:

$$\frac{d}{dx}\left(p_{n-1}(x)\right)=0 \tag{5}$$

Once the nodes x_i are known, the weight coefficients w_i can be found as:

$$w_j=\frac{2}{n(n-1)\left[p_{n-1}(x_j)\right]^2},x\neq\pm1 \tag{6}$$

where the error is expressed as [16].

$$E(f) = -\frac{n(n-1)^3 2^{2n-1}[(n-2)!]^4}{(2n-1)[(2n-2)!]^3} f^{(2n-2)}(\xi), -1 < \xi < 1 \tag{7}$$

Since equation (4) is defined at an interval between [−1, 1], a change of variable can be used to apply the quadrature to a general interval between [*a*, *b*]. When considering the change of variable $t = (a+b)dt/2 + (b-a)x/2$, with $dt = (a-b)dx/2$. In this way, the quadrature scheme becomes [17]:

$$\int_a^b f(t)dt = \frac{b-a}{n(n-1)}[f(a) - f(b)] + \frac{b-a}{2}\sum_{j=2}^{n-1} w_j f\left(\frac{(b-a)x_j + a + b}{2}\right) + \frac{b-a}{2}E(f) \tag{8}$$

With equation (8), a compound quadrature rule can be constructed by dividing the integration interval [*a*, *b*] into a number *z* of small subintervals of size Δt where the integral will be evaluated in each subinterval to ultimately add all the evaluations and thus obtain the value of the integral over the entire interval as shown in equation (9)

$$\int_0^{t_f} f(t)dt = \int_0^{\Delta t} f(t)dt + \int_{\Delta t}^{2\Delta t} f(t)dt + \ldots + \int_{k\Delta t}^{(k+1)\Delta t} f(t)dt = \sum_{k=0}^{z-1}\int_{k\Delta t}^{(k+1)\Delta t} f(t)dt \tag{9}$$

The integration interval [t_0, t_f] is discretized such that $t_0 = 0$ and $t_f = z\Delta t$, then we apply the variable transformation shown in equation (8) to each term in equation (9) within the limits $a = k\Delta t$ and $b = (k+1)\Delta t$ where $0 \le k < z$. Consequently, the compound quadrature rule is formulated as shown in equation (10),

$$\int_0^{t_f} f(t)dt = \sum_{k=0}^{z-1}\left[\frac{\Delta t}{n(n-1)}(f(k\Delta t) + f((k+1)\Delta t)) + \frac{\Delta t}{2}\sum_{j=2}^{n-1} w_j f\left(\frac{\Delta t}{2}(x_j + 2k + 1)\right) - \frac{n(n-1)^3 2^{2n-1}[(n-2)!]^4}{(2n-1)[(2n-2)!]^3} f^{(2n-2)}(\xi)\right] \tag{10}$$

where the error term also moves in the interval $k\Delta t < \xi < (k+1)\Delta t$. The notation of equation (10) can be simplified by considering that the sum of nodes and weights takes the values $w_1 = w_n = 2/n(n-1)$ $x_1 = -1, x_n = 1$. In this way, once these conditions are established and neglecting the error term, the quadrature scheme of equation (10) can be applied to an integral part of equation (3), resulting in:

$$\int_0^t e^{-\lambda_i(t-t')}N(t')dt' \approx \frac{\Delta t}{2}\sum_{k=0}^{z-1} \times \sum_{j=1}^{n} w_j e^{-\lambda_i\left(t - \frac{\Delta t}{2}(x_j + 2k + 1)\right)} N\left(\frac{\Delta t}{2}(X_J = 2K = 1)\right) \tag{11}$$

The expression obtained in equation (11) is replaced in equation (3). Then, the corresponding discretization is carried out in the temporal variable. This changes a continuous scheme to a discrete one where only the values of the neutron density at points given by the nodes of the Gauss-Lobatto quadrature are needed.

$$\rho(t_z) \approx \beta + \frac{\Lambda}{N(t_z)}\frac{dN(t_z)}{dt} - \frac{\langle N_0\rangle}{N(t_z)}\sum_{i=1}^{m}\beta_i e^{-\lambda_i t_z} - \frac{\Delta t}{2N(t_z)} \times \sum_{i=1}^{m}\sum_{k=0}^{z-1}\sum_{j=1}^{n}\lambda_i\beta_i w_j e^{-\lambda_i\left(t_z - \frac{\Delta t}{2}(x_j + 2k + 1)\right)} \times N\left(\frac{\Delta t}{2}(x_j + 2k + 1)\right) \tag{12}$$

The triple summation of equation (12) can be simplified if a new temporal vector is constructed, given by the evaluation of the nodes of the quadrature $t_{n\ k+j} = (x_j + 2k + 1)\,\Delta t/2$, where $t_z = t_{nz}$, with this, a vector that contains the information related to the six groups of precursors can be constructed, as shown in equation (13):

$$h\left(t_{n\ k+j}\right) = \sum_{i=1}^{m}\lambda_i\beta_i e^{-\lambda_i\left(t_{n\ k+j}\right)}. \tag{13}$$

Once equation (13) is constructed, it is necessary to incorporate the weights w_j given by the quadrature,

$$H\left(t_{n\ k+j}\right) = w_j\, h\left(t_{n\ k+j}\right) = w_j\sum_{i=1}^{m}\lambda_i\beta_i e^{-\lambda_i\left(t_{n\ k+j}\right)} \tag{14}$$

In this way, a substitution is made such that $s = nk + j$, in which *s* is defined between $1 \le s \le nz$. Thus, substituting equation (14) into equation (12) and considering that $t_z = t_{nz}$, it is possible to obtain the expression shown in (15),

$$\rho(t_{nz}) \approx \beta + \frac{\Lambda}{N(t_{nz})}\frac{dN(t_{nz})}{dt} - \frac{\langle N_0\rangle}{N(t_{nz})}\sum_{i=1}^{m}\beta_i e^{-\lambda_i t_{nz}} - \frac{\Delta t}{2N(t_{nz})}\sum_{s=1}^{nz}H(t_{nz}-t_s)N(t_s) \tag{15}$$

The triple sum shown in equation (12) is a convolution product but is different due to the weights w_i given by the quadrature. The convolution term of equation (15) can be interpreted as the product between the impulse response $H(t)$ and the neutron population density $N(t)$.

3.1. Differential scheme

A differential scheme is proposed to take advantage of the nodes given by the Gauss-Lobatto quadrature. Different applications have been solved using fractional derivatives [18]. However, in this paper, we do not consider such development. The neutron population density is approximated with a Lagrange interpolating polynomial passing through the nodes, as shown in equation (16),

$$N(t_z) \approx \sum_{i=1}^{m}\prod_{\substack{j=1\\ j\neq i}}^{n}\frac{t-t_j}{t_i-t_j}N(t_i). \tag{16}$$

Once the interpolating polynomial has been constructed for the neutron population density, it is possible to derive equation (16), thus obtaining:

$$\frac{d}{dt}N(t_z) \approx \sum_{i=1}^{m}N(t_i)\frac{d}{dt}\left(\prod_{\substack{j=1\\ j\neq i}}^{n}\frac{t-t_j}{t_i-t_j}\right)_{t=t_z}. \tag{17}$$

When evaluating equation (17), considering that $t_j = t_{n\,z+j} = z\Delta t + (x_j + 1)\Delta t/2$, a scheme for the numerical derivative that uses the nodes given by the quadrature can be obtained, as shown in equation (18),

$$\frac{d}{dt}N(t_z) = \frac{1}{\Delta t}\sum_{j=1}^{n}u_j N\left(t_{n\,z+j}\right), \tag{18}$$

In which u_j are the weight coefficients that result from implementing the differential scheme proposed in equation (17).

If the differential quadrature obtained in equation (18) is substituted into the equation of interest given in equation (15), a numerical expression is finally obtained to calculate nuclear reactivity.

$$\rho(t_k) = \beta + \frac{\Lambda}{N(t_k)}\frac{1}{\Delta t}\sum_{j=1}^{n}u_j N\left(t_{k+j}\right)\frac{\langle N_0\rangle}{N(t_k)}\sum_{i=1}^{m}\beta_i e^{-\lambda_i tk} + \frac{\Delta t}{2N(t_k)}\sum_{s=1}^{k}H(t_k-t_s)N(t_s) \tag{19}$$

where $k = nz$ ($z = 1, 2, 3, \ldots$) The nuclear reactivity equation, shown in equation (19), can be solved by knowing the density of the neutron population within the reactor core.

This information can be obtained using measurement sensors such as ionization chambers or fission chambers. The data obtained by these instruments may exhibit fluctuations caused by oscillations within the reactor, such as displacement of core components and changes in temperature or density. Additionally, detection noise generated by the measurement equipment [3] may also contribute to these fluctuations.

For this work, it is assumed that these fluctuations can be represented by a multiplicative Gaussian white noise around a mean value, as shown in equation (20).

$$NP(t) = \overline{N}(t) + \sigma\overline{N}(t)\,\xi(t), \tag{20}$$

where $NP(t)$ is the density of the perturbed neutron population, $\overline{N}(t)$ is the average population density, $\xi(t)$ is white noise and σ refers to the magnitude of the deviations introduced.

The fluctuations in $NP(t)$ can be reduced by means of a low-pass filter to reduce their impact on the calculation of nuclear reactivity. As consequence of such filtering, $NP(t)$ is expected to be approximately equal to $N(t)$.

3.2. Butterworth filter design

The Butterworth filter is a type IIR (infinite impulse response) filter with a flat maximum frequency response throughout the passband. The transfer function of a second-order low-pass Butterworth filter can be written as in equation (21) [19],

$$H(s) = \frac{1}{s^2 + \sqrt{2}s + 1}, \tag{21}$$

where s represents the complex plane where the transfer functions of the analog filter are defined. In order to take equation (21) to a digital format, we apply the bilinear transform,

$$s = \frac{1}{c}\frac{1-z^{-1}}{1+z^{-1}}, \tag{22}$$

where the Z-transform gives a complex number, c is a positive constant that can be set to map from an analog frequency to a digital frequency.

In the case of a low-pass filter, c is typically used to adjust the cut-off frequency to be identical in analog and digital cases.

The nonlinear relationship between the analog angular cut-off frequency and the digital angular cut-off frequency produced by the bilinear transformation can be determined by evaluating in equation (22), thus obtaining an expression as shown in equation (23) [20].

$$w_a = \frac{1}{c}\tan\left(\frac{w_c T}{2}\right), \tag{23}$$

where $T = 1/f_s$ is the sampling period, f_s refers to the sampling frequency (Hz), $w_c = 2\pi f_c$ with f_c being the cut-off frequency (Hz).

Furthermore, to find an appropriate value of c, a normalization condition is established when $w_a = 1$, and by solving for c in equation (23), we obtain equation (24),

$$c = \tan\left(\frac{\pi f_c}{f_s}\right). \tag{24}$$

Now, if equation (22) is substituted back into equation (21), it results:

$$H(z) = \frac{1}{\left(\frac{1}{c}\frac{1-z^{-1}}{1+z^{-1}}\right)^2 + \sqrt{2}\left(\frac{1}{c}\frac{1-z^{-1}}{1+z^{-1}}\right) + 1}, \tag{25}$$

By developing the expressions in equation (25), we can write:

$$H(z) = \frac{\left(\frac{c^2}{c^2+\sqrt{2}c+1}\right)(1+2z^{-1}+z^{-2})}{1+\frac{2c^2-2}{c^2+\sqrt{2}c+1}z^{-1}+\frac{c^2-\sqrt{2}c+1}{c^2+\sqrt{2}c+1}}, \tag{26}$$

If equation (26) is compared with a transfer function of a second-order digital filter, the following coefficients can be obtained [21],

$$\begin{aligned} b_0 = b_2 = \frac{c^2}{c^2+\sqrt{2}c+1}, b_1 = 2b_0 \\ a_0 = 1, a_1 = \frac{2c^2-2}{c^2+\sqrt{2}c+1}, a_2 = \frac{c^2-\sqrt{2}c+1}{c^2+\sqrt{2}c+1}, \end{aligned} \tag{27}$$

The parameters b_i and a_i are the coefficients that control the characteristics of the digital filter.

Once the coefficients in equation (27) have been determined, a second-order difference equation is constructed to carry out the filtering process as follows:

$$\begin{aligned} y[k] = b_0 x[k] + b_1 x[k-1] + b_2 x[k-2] - a_1 y[k-1] \\ - a_2 y[k-2], \end{aligned} \tag{28}$$

here y [k] is the filtered output signal that is obtained as a linear combination of present x [k] and past inputs (signal with fluctuations) minus a linear combination of past outputs (feedback term).

If a signal with fluctuations is considered, as in equation (20), equation (28) can be written as:

$$\begin{aligned} Nf[k] = b_0 NP[k] + b_1 NP[k-1] + b_2 NP[k-2] \\ - a_1 Nf[k-1] - a_2 Nf[k-2] \end{aligned} \tag{29}$$

where **Nf** [**k**] is the filtered signal at the instant k and NP [k] is the density of the perturbed neutron population given by equation (20).

Equation (29) generates a delay of two samples, which implies that to filter the first sample in Nf [t_1], it is necessary to know the filtering of the two previous samples.

These samples can be determined by setting the first and second filtered samples equal to the initial condition of the neutron population density Nf [t_{-1}] = Nf [t_0] = N_0.

4. Results

This section shows results from different numerical experiments using the Gauss-Lobatto quadrature and the Butterworth filter in the presence of noise given by equation (20) with a seed generating random numbers of $2^{31}-1$ and standard deviations (σ) between [0.01, 0.1].

The numerical simulations are carried out considering a quadrature of three (Glo-3) and four (Glo-4) points, which result when implementing $n = 3$ and $n = 4$, correspondingly, in equation (4).

The physical parameters of a thermal reactor that uses Uranium-235 as fuel are considered [22]. The physical values for these parameters are β_i = {0.000266, 0.001491, 0.001316, 0.002849, 0.000896, 0.000182}, $\beta = \sum\beta_i = 0.007$, λ_i = {0.0127, 0.0317, 0.115, 0.311, 1.4, 3.87} s^{-1} and $\Lambda = 2 \times 10^{-5}$ s.

The passage of time in the calculation of reactivity varies between $\Delta T = 0.1$ s and $\Delta T = 0.01$ s where the total simulation time of each numerical experiment is T = 1000 s, T = 800 s, T = 5 00 s, T = 600 s, T = 150 s, T = 60 s for ω = 0.00243 s^{-1}, ω = 0.006881 s^{-1}, ω = 0.01046 s^{-1}, ω = 0.02817 s^{-1}, ω = 1.00847 s^{-1}, ω = 11.6442 s^{-1}, and T = 300 s for $\omega \geq$ 0.12353 s^{-1}, with ω being the roots of the *inhour*

equation, it is for the exponential density of the neutron population [22].

The Butterworth filter is taken as second order in the filtering process with a sampling window $M = 3$. The exact solution of equation (3) is used as a reference to validate the efficiency of the proposed method with the Butterworth filter, where the density of the neutron population $N(t)$ is assumed to be known and without fluctuations. Another way to validate the efficiency of the Butterworth filter process is to use common quadratures. For this reason, a Savitzky–Golay (SGF) filter that uses a Gram polynomial of order $d = 2$ with a sampling window of $M = 225$ was implemented [23]. In addition, the need to carry out a filtering process on the neutron population density to calculate nuclear reactivity is also shown when comparing the results of the proposed method when no filtering process is carried out.

Since the Butterworth and the Savitzky–Golay (SGF) filters need several M samples to start the filtering process, in all numerical experiments, M samples are discarded at the beginning and end of each simulation to compare them. This is because in the SGF filter, the delay time introduced is $M\,\Delta T$.

For all numerical experiments presented in this work, a neutron population density of the form $N(t) = \exp(\omega t)$ was considered for different values of ω. Results shown are in pcm (parts per hundred thousand) to maximize the differences in reactivity, MDR, and absolute mean errors.

Tables 1 and 2 show results for mean absolute errors with $\Delta T = 0.1$ s and $\sigma = 0.1$ and $\sigma = 0.01$, in the given order. Six columns of results are shown; the first two correspond to the calculation of reactivity with a three-point quadrature, Glo-3, and a four-point quadrature, Glo-4, when no filtering process is carried out on the neutron population density. The following two columns correspond to the validation method, which uses the SGF filter with a window width of $M = 225$ samples to calculate the reactivity with the Glo-3 and Glo-4 quadratures. Finally, the last two columns correspond to the results of the proposed method, which implements the three- and four-point Gauss-Lobato quadratures and the second-order Butterworth filter, BTW, with a window width of $M = 3$ samples for calculating nuclear reactivity.

The results show that the BTW filter with three samples produces consistent results of a similar order of magnitude to the FSG filter, which uses 225 samples. However, it does introduce a delay of 22.5 s.

Additionally, a significant improvement in the results is observed when a filtering process is implemented, compared to those presented in Glo-3 and Glo-4. The cut-off frequencies for these experiments were $f_c = 0.03\ s^{-1}$ for $\omega \leq 0.01046\ s^{-1}$, $f_c = 0.024\ s^{-1}$, $f_c = 0.042\ s^{-1}$, $f_c = 0.45\ s^{-1}$ for $\omega = 0.02817\ s^{-1}$, $\omega = 0.12353\ s^{-1}$, $\omega \leq 1.00847\ s^{-1}$ respectively.

The numerical experiments in Tables 3 and 4 show the maximum differences and mean absolute error for $\Delta T = 0.01$ s with $\sigma = 0.01$.

These results show that in the case of the Glo-3 and Glo-4 quadratures, when the BWT filter is used, their results are similar. It is also evident that the absolute mean values for $\omega \leq 0.016957\ s^{-1}$ the method improves the results. However, in the maximum differences, the method presents results like those obtained with the FSG filter. It is also

Table 1. Mean absolute error for $\Delta T = 0.1$ s and $\sigma = 0.1$.

$N(t) = exp(\omega t)$	Glo-3	Glo-4	Fsg-3	Fsg-4	Btw-3	Btw-4
$\omega = 0.00243$	61.12	67.14	3.55	3.99	2.84	3.20
$\omega = 0.00688$	58.56	64.72	3.27	3.71	2.71	3.06
$\omega = 0.01046$	57.18	63.59	3.04	3.36	2.78	2.93
$\omega = 0.02817$	51.64	57.92	2.57	2.89	2.56	4.95
$\omega = 0.12353$	38.61	46.20	1.82	1.76	3.81	3.40
$\omega = 1.00847$	19.07	26.32	2.86	33.50	3.53	3.80

Table 2. Mean absolute error for $\Delta T = 0.1$ and $\sigma = 0.01$.

$N(t) = exp(\omega t)$	Glo-3	Glo-4	Fsg-3	Fsg-4	Btw-3	Btw-4
$\omega = 0.00243$	5.98	5.74	0.35	0.39	0.33	0.34
$\omega = 0.00688$	5.73	6.34	0.32	0.41	0.45	0.37
$\omega = 0.01046$	5.61	6.25	0.30	0.33	0.70	0.56
$\omega = 0.02817$	5.06	5.68	0.25	0.25	0.67	0.67
$\omega = 0.12353$	3.80	4.53	0.17	0.20	0.94	0.85
$\omega = 1.00847$	1.87	2.58	0.28	2.65	0.65	1.17

Table 3. Maximum differences for $\sigma = 0.01$ and $\Delta T = 0.01$ s.

$N(t) = exp(\omega t)$	Glo-3	Glo-4	Fsg-3	Fsg-4	Btw-3	Btw-4
$\omega = 0.00243$	77.88	126.04	2.75	2.67	1.51	1.59
$\omega = 0.00688$	76.42	124.85	2.63	2.47	2.54	2.02
$\omega = 0.01046$	124.05	75.45	2.55	2.40	3.57	2.73
$\omega = 0.02817$	72.03	121.25	2.27	2.24	5.90	4.48
$\omega = 0.016957$	73.98	122.85	2.43	2.34	3.55	2.89
$\omega = 0.12353$	64.25	114.85	1.62	1.74	5.78	5.25
$\omega = 1.00847$	47.20	95.16	0.94	2.05	7.82	7.07

Table 4. Mean absolute error for $\sigma = 0.01$ and a $\Delta T = 0.01$ s.

$N(t) = exp\ (\omega t)$	Glo-3	Glo-4	Fsg-3	Fsg-4	Btw-3	Btw-4
$\omega = 0.00243$	12.17	20.53	0.50	0.52	0.33	0.34
$\omega = 0.00688$	12.00	20.41	0.47	0.50	0.32	0.33
$\omega = 0.01046$	20.37	11.87	0.45	0.47	0.34	0.33
$\omega = 0.02817$	11.42	19.98	0.40	0.43	0.39	0.38
$\omega = 0.016957$	11.67	20.20	0.43	0.45	0.43	0.43
$\omega = 0.12353$	10.43	19.06	0.29	0.33	0.84	0.93
$\omega = 1.00847$	8.95	17.79	0.12	1.24	0.74	1.61

evident that for $\omega \leq 0.016957\ s^{-1}$ the method improves the absolute mean values. However, in the maximum differences the method presents similar results to those obtained with the FSG filter. For these experiments the cut-off frequencies are $f_c = 0.215\ s^{-1}$ for $\omega \leq 0.01046\ s^{-1}$, $f_c = 0.35\ s^{-1}$, $f_c = 0.4\ s^{-1}$, $f_c = 3\ s^{-1}$ and $f_c = 7\ s^{-1}$ for the other values of ω, respectively.

Tables 5 and 6 present the maximum differences and the mean absolute error with a $\sigma = 0.1$ and a step size of $\Delta T = 0.01$ s. The results show that for $\sigma = 0.1$ when no filtering is applied (Glo-3 and Glo-4), the errors are considerably high in both maximum differences and mean error compared to when a filtering process is applied using the SGF and BWF filters, where it can be noted that the errors are significantly reduced.

Additionally, it can be observed that the proposed method, when using the BWF, produces lower maximum differences and mean errors in the reactivity calculation when compared to the SGF. In these experiments, the cut-off frequencies were $f_c = 0.215\ s^{-1}$ for $\omega \leq 0.01046\ s^{-1}$, $f_c = 0.35\ s^{-1}$, and $f_c = 0.4\ s^{-1}$ for the other values of ω, respectively.

Fig. 1 shows the behavior of the nuclear reactivity calculation with the three-point quadrature and the Butterworth filter, Glo-3+BTW, compared to the reference method. A maximum difference of 3.5556 pcm and a mean error of 0.47 pcm are achieved for a time step size $\Delta T = 0.01$ s and $\sigma = 0.01$.

Fig. 2 shows the behavior of the error in the calculation of nuclear reactivity with the same simulation parameters as in Fig. 1. It is evident that the maximum difference was obtained in the first moments of the simulation, since every filter has a characteristic stability and a memory process as represented in equation (29), after filtering, the method stabilizes and the errors decrease, showing an average error of 0.47 pcm.

Table 5. Maximum differences for $\Delta T = 0.01$ s y $\sigma = 0.1$.

$N(t) = exp(\omega t)$	Glo-3	Glo-4	Fsg-3	Fsg-4	Btw-3	Btw-4
$\omega = 0.00243$	1389.4	1961.0	28.54	26.70	14.85	15.56
$\omega = 0.00688$	1363.2	1942.4	27.31	25.62	13.52	14.82
$\omega = 0.01046$	1345.9	1930.0	26.49	24.88	13.04	13.73
$\omega = 0.02817$	1285.0	1886.5	23.59	22.26	16.88	17.94
$\omega = 0.016957$	1319.8	1911.4	25.25	23.77	19.64	20.65

Table 6. Mean absolute error for $\Delta T = 0.01$ s and $\sigma = 0.1$.

$N(t) = exp(\omega t)$	Glo-3	Glo-4	Fsg-3	Fsg-4	Btw-3	Btw-4
$\omega = 0.00243$	123.85	208.27	5.06	5.26	3.33	3.43
$\omega = 0.00688$	122.05	207.02	4.75	5.01	3.10	3.28
$\omega = 0.01046$	120.66	206.76	4.57	4.78	3.01	3.09
$\omega = 0.02817$	116.04	202.81	4.04	4.33	3.51	3.69
$\omega = 0.016957$	118.67	205.00	4.35	4.56	4.10	4.19

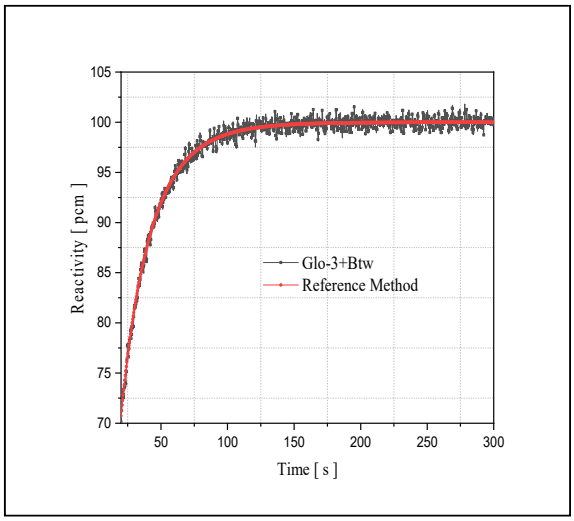

Fig. 1. Numerical reactivity for $\omega = 0.016957\ s^{-1}$.

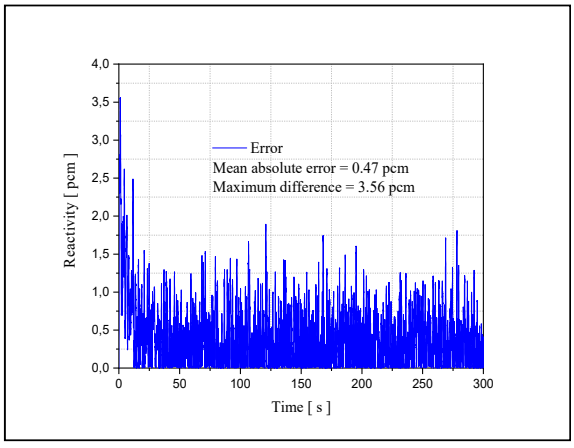

Fig. 2. Error in the nuclear reactivity calculation Numerical reactivity.

5. Conclusions

A method was presented to reduce fluctuations in the calculation of nuclear reactivity using the inverse equation of point kinetics. The proposed method is based on the Gauss-Lobatto quadrature with $n = 3$ and $n = 4$ points that uses a Legendre polynomial of degree $n - 1$ to approximate the integral contained in the IKPE.

To reduce fluctuations, a second-order low-pass Butterworth filter that uses only three samples was used to carry out the filtering process if the density of the neutron population within the reactor core presents a Gaussian noise distribution around a mean value. From the results it is possible to notice that fluctuations in nuclear reactivity can be reduced

with the Butterworth filter, showing that the filter turns out to be very useful for different time step sizes and standard deviations when compared to a filter that uses a greater number of samples such as the Savitzky–Golay filter with $M = 225$ samples that produces a greater delay in the calculation of reactivity.

Ethics information

All research activities complied with relevant ethical standards for studies without human or animal subjects.

Funding

The authors did not receive support from any organization for the submitted work.

Acknowledgements

Two authors (DSD and LeCP) thank the research seed of Computational Physics, the research group in Applied Physics FIASUR at the Surcolombiana University, Neiva, Colombia.

References

[1] J.J. Duderstadt, L.J. Hamilton, Nuclear Reactor Analysis, Wiley, New York. 1976.
[2] J.C. Lee, Nuclear Reactor Physics and Engineering, Wiley, New York. 2020.
[3] B. Yuan, S. Guo, W. Yang, S. Zhang, B. Zhong, J. Wei, Y. Ying, Time-frequency analysis of reactor neutron noise under bubble disturbance and control Rod Vibration, Nucl. Eng. Technol. 53 (2021) 1088–1099, https://doi.org/10.1016/j.net.2020.10.003.
[4] J. Hyvärinen, J. Vihavainen, M. Ylönen, J. Valkonen, An overall safety concept for nuclear power plants, Ann. Nucl. Energy 178 (2022) 109353, https://doi.org/10.1016/j.anucene.2022.109353.
[5] F. Xiang, Y. He, Y. Wu, Y. Niu, S. Qiu, C. Tang, K. Wang, W. Tian, G. Su, Investigation of plate fuel performance under reactivity initiated accidents with developed multi-dimensional coupled method, J. Nucl. Mater. 583 (2023) 154537, https://doi.org/10.1016/j.jnucmat.2023.154537.
[6] N. Hossain, M.A. M Soner, M.M. H Prodhan, M. H Sahadath, K.A. Kabir, Experimental analysis of step reactivity insertion effect on reactor power, fuel temperature and reactor period in BAEC TRIGA research reactor, Ann. Nucl. Energy 165 (2022) 108665, https://doi.org/10.1016/j.anucene.2021.108665.
[7] W. Jiang, Q.F. Zhu, Q. Zhou, F. Ma, L. Zhang, Y. Liu, J.Y. Li, H.L. Ge, R. Yu, H.Y. Meng, D.W. Wang, L. Chen, Reactivity worth measurement of the lead target on VENUS-II light water reactor and validation of evaluated nuclear data, Ann. Nucl. Energy 165 (2022) 108779, https://doi.org/10.1016/j.anucene.2021.108779.
[8] V.A. Vasilenko, A.M. Pankin, K.V. Skvortsov, Reactivity calibrator, Atom. Energy 125 (2019) 157–161, https://doi.org/10.1007/s10512-018-00459-0.
[9] V.E. Zhitarev, V.M. Kachanov, A. Yu. Sergevnin, N.E. Sutemieva, Correction of the reactivity measured by ORUK Technique, Phys. Atom. Nucl. 84 (2021) 1405–1412, https://doi.org/10.1134/S1063778821080214.
[10] J. Li, Q. Zhou, Y. Xia, J. Mou, R. Zhai, Z. Shen, B. Lin, Study on reactivity control strategies for the thermo-electric integrated space nuclear reactor, Ann. Nucl. Energy 145 (2020) 107607, https://doi.org/10.1016/j.anucene.2020.107607.
[11] G. Chiba, J. Fan, Experimental analysis of small sample reactivity measured in the SEG experiment by a deterministic reactor physics code system CBZ, J. Nucl. Sci. Technol. 59 (2022) 247–256, https://doi.org/10.1080/00223131.2021.1958084.
[12] D. Suescún-Díaz, G. Ule-Duque, L.E. Cardoso-Páez, Butterworth filter to reduce reactivity fluctuations, Karbala Int. J. Modern Sci. 10 (2024) 91–98, https://doi.org/10.33640/2405-609X.3342.
[13] W.M. Stacey, Nuclear Reactor Physics, Wiley, Weinheim. 2018.
[14] S. Marguet, The Physics of Nuclear Reactors, Springer, Switzerland. 2017.
[15] H. Dehestani, Y. Ordokhani, an efficient approach based on Legendre–Gauss–Lobatto quadrature and discrete shifted Hahn polynomials for solving Caputo–Fabrizio Fractional Volterra partial integro-differential equations, J. Comput. Appl. Math. 403 (2022) 113851, https://doi.org/10.1016/j.cam.2021.113851.
[16] P.J. Davis, P. Rabinowitz, Methods of Numerical Integration, Elsevier Science, Kent. 2014.
[17] K.J. Beers, Numerical Methods for Chemical Engineering: Applications in MATLAB, Cambridge University Press, Cambridge. 2009.
[18] M.H. Heydari, M. Razzaghi, Jacobi polynomials method for a coupled system of Hadamard fractional Klein–Gordon–Schrödinger equations, Alex. Eng. J. 107 (2024) 73–86, https://doi.org/10.1016/j.aej.2024.07.016.
[19] X. Meng, H. Tian, X. Chen, X. Jiang, P. Wang, T. Wei, G. Cai, Numerical simulation of combustion surface regression based on Butterworth filter in hybrid rocket motor, Acta Astronaut. 202 (2023) 400–410, https://doi.org/10.1016/j.actaastro.2022.11.003.
[20] A. Akan, L.F. Chaparro, Signals and Systems Using MATLAB, Elsevier, Academic Press, London. 2024.
[21] L. Tan, J. Jiang, Digital Signals Processing: Fundamentals and Applications, Academic Press. 2018.
[22] M. Kinard, E.J. Allen, Efficient numerical solution of the point kinetics equations in nuclear reactor dynamics, Ann. Nucl. Energy 31 (2004) 1039–1051, https://doi.org/10.1016/j.anucene.2003.12.008.
[23] D. Suescún-Díaz, G. Ule-Duque, J.A. Chala-Casanova, Reduction of fluctuations in the calculation of nuclear reactivity using the Gauss-Legendre quadrature with a Savitzky-Golay filter, Nucl. Eng. Des. 413 (2023) 112565, https://doi.org/10.1016/j.nucengdes.2023.112565.